PERGAMON

Available online at www.sciencedirect.com

SCIENCE DIRECT®

Automatica 39 (2003) 1019–1025

automatica

www.elsevier.com/locate/automatica

Brief Paper

Open-loop worst-case identification of nonSchur plants☆

Mario Sznaier*, Cecilia Mazzaro, Octavia Camps

Department of Electrical Engineering, The Pennsylvania State University, University Park, PA 16802, USA

Received 20 December 2001; received in revised form 30 September 2002; accepted 30 January 2003

Abstract

This paper presents an LMI based algorithm for deterministic worst-case identification of nonSchur plants in an open-loop setting. Contrary to other approaches dealing with this problem, the proposed technique does not require prior knowledge of a stabilizing controller. The main result of the paper shows that, as the information is completed, the identified model converges, in the ℓ_2-induced topology, to the actual plant. Additional results include upper bounds on the worst-case identification error on the finite horizon. The usefulness of the proposed approach is illustrated with a practical example arising in the context of robust visual tracking.

Keywords: Robust identification; Open-loop identification; Visual tracking

1. Introduction

The problem of identifying nonSchur (i.e. marginally stable or unstable) plants has been addressed several times in the literature (see the survey by Mäkilä, Partington, & Gustafsson, 1995). A common feature of all these papers is that they require prior knowledge of a controller that will stabilize the unknown plant. Working in an $\mathscr{H}_\infty$ setting, and under the additional assumption that the unknown plant is strongly stabilizable, Mäkilä and Partington (1992) showed that this approach leads to an approximation to the *open loop* unstable plant that converges in the graph, gap and chordal metrics. The existence of robustly convergent algorithms in the ℓ_1 sense and bounds on the identification error were obtained in Partington and Mäkilä (1994).

Alternatively, by considering the unknown plant as a member of the set of all plants stabilized by the known controller, the problem can be reduced to the identification of a stable system, namely the Youla–Kucera parameter. This approach was proposed by Hansen, Franklin, and Kosut (1989) and Schrama (1991), and extended by Dasgupta and Anderson (1996) to nonlinear time varying plants.

While successful, these approaches are limited by the assumption that a stabilizing controller is known. This requirement can be too restrictive, for instance in cases where the plant is not strongly stabilizable (and thus the controller itself has to be open loop unstable). Moreover, as we illustrate in the sequel with a problem arising in the context of computer vision, many practical problems involve estimating marginally stable dynamics that cannot be stabilized.

To avoid these difficulties, in this paper we directly identify the plant from some a priori assumptions and time-domain measurements of its output over a finite horizon $[0, N]$. Note that in the case of marginally stable or mildly unstable plants, it is feasible to carry out these time-domain experiments over reasonably long horizons. Formally, the proposed approach is similar to the one used by Chen and Nett (1995) and Parrilo, Sánchez Peña, and Sznaier (1999) for worst-case identification of stable plants. The main result of this paper shows that *even when used for open-loop unstable plants*, the identification algorithm converges in the ℓ_2-induced topology as the information is completed, i.e. as the noise level tends to zero and the number of data points to infinity. In addition, we provide worst-case identification error bounds over a finite horizon. The usefulness of the proposed approach is illustrated with an academic example and a practical one, that involves robustly tracking a person in a sequence of video frames.

☆This paper was not presented at any IFAC meeting. This paper was recommended for publication in revised form by Associate Editor Toshiharu Sugie under the direction of Editor Roberto Tempo.

* Corresponding author. Tel.: 814-865-0196; fax: 814-865-7065.

E-mail addresses: msznaier@gandalf.ee.psu.edu (M. Sznaier), cmazzaro@gandalf.ee.psu.edu (C. Mazzaro), camps@whale.ee.psu.edu (O. Camps).

0005-1098/03/$ - see front matter © 2003 Elsevier Science Ltd. All rights reserved.
doi:10.1016/S0005-1098(03)00061-X

2. Notation

This paper considers discrete time, single input–single output, causal, linear time invariant (LTI) systems represented by the convolution kernel $y_k = (h * u)_k \doteq \sum_{j=0}^{k} h_{k-j}u_j$, or, alternatively by the complex-valued transfer function $H(z) = \sum_{k=0}^{\infty} h_k z^{-k}$.

$\mathscr{H}_{\infty,\rho}$ denotes the space of complex-valued functions $H(z)$ essentially bounded on $|z| = \rho$ and with bounded analytic continuation in $|z| > \rho$, equipped with the usual norm $\|H\|_{\infty,\rho} \doteq \sup_{|z|>\rho} |H(z)|$. $\mathscr{B}\mathscr{H}_{\infty,\rho}(K)$ denotes the closed K-ball in $\mathscr{H}_{\infty,\rho}$. In the sequel, we will use simply $\mathscr{H}_\infty$ and $\|\cdot\|_\infty$ for the case $\rho = 1$ and $\mathscr{B}\mathscr{H}_\infty$ for the closed unit ball.

$\ell_2[0,N]$ denotes the space of square summable, real-valued sequences $\{x_i\}_{k=0}^{N}$ equipped with the norm $\|x\|^2_{\ell_2[0,N]} \doteq \sum_{i=0}^{N} x_i^2 < \infty$. Similarly, $\ell_\infty[0,N]$ denotes the space of bounded sequences equipped with the norm $\|x\|_{\ell_\infty[0,N]} \doteq \sup_{0\leqslant i\leqslant N} |x_i| < \infty$ and $\mathscr{B}\ell_\infty(N,\varepsilon)$, the origin centered ε radius closed ball in this space. $\|h\|_{\ell_2[0,N]\to\ell_2[0,N]}$ denotes the ℓ_2 induced norm in $\mathscr{L}(N)$, the space of causal, LTI operators bounded in $\ell_2[0,N]$. The projection operator $\mathscr{P}_N$ is defined by $\mathscr{P}_N[h] \doteq \{h_0, h_1, \ldots, h_N, 0, 0, \ldots\}$. To a given sequence x, we will associate the column vector $\mathbf{x}$ and the finite lower Toeplitz matrix $\mathbf{T}_x$:

$$\mathbf{x} \doteq \begin{bmatrix} x_0 \\ \vdots \\ x_N \end{bmatrix}, \quad \mathbf{T}_x \doteq \begin{bmatrix} x_0 & \cdots & 0 \\ \vdots & \ddots & \vdots \\ x_N & \cdots & x_0 \end{bmatrix}.$$

Given a subset $\mathscr{A}$ of a metric space $(\mathscr{X}, m)$ its diameter is defined as $d(\mathscr{A}) \doteq \sup_{x,a\in\mathscr{A}} m(x,a)$ and $\bar{\mathscr{A}}$ denotes its closure. Finally, given a matrix $\mathbf{M}$, $\mathbf{M}^{\mathrm{T}}$ denotes its transpose, $\mathbf{M}^{\dagger}$ its Moore–Penrose pseudoinverse, $(\mathbf{M})_i$ its ith row and $\|\mathbf{M}\|_1 = \max_i \sum_j |(\mathbf{M})_{i,j}|$. As usual, $\mathbf{M} > 0 (\mathbf{M} \geqslant 0)$ indicates that $\mathbf{M}$ is positive definite (positive semi-definite).

3. Identification of nonSchur plants

3.1. Problem statement

Consider the problem of identifying a nonSchur plant g from measurements of its output y to a known input $u \in \ell_2[0,N]$, corrupted by additive bounded noise η:

$$y_k = (g * u)_k + \eta_k, \quad k = 0, 1, \ldots, N,$$

$$\eta \in \mathscr{N} \doteq \mathscr{B}\ell_\infty(N,\varepsilon).$$

Further, the plant is known to belong to a given set of candidate models $\mathscr{S}$:

$$\mathscr{S} \doteq \{G(z) = H(z) + P(z)\}.$$

Here $H(z)$ denotes the nonparametric component of the model, in a given set $\mathscr{S}_{np}$ to be defined later. On the other hand, $P(z)$ represents the parametric component and is assumed to belong to the following class $\mathscr{P}$ of affine models:

$$\mathscr{P} \doteq \{P(z) = \mathbf{p}^{\mathrm{T}}\mathbf{G}_p(z), \mathbf{p} \in \mathscr{R}^{N_p}\},$$

where the N_p components $\mathbf{G}_{p_i}(z)$ of vector $\mathbf{G}_p(z)$ are known, linearly independent, rational transfer functions.

The identification problem can be precisely stated as follows.

Problem 1. Given an unknown nonSchur plant g, the a prior sets of candidate models and noise $(\mathscr{S}, \mathscr{N})$ and a finite set of samples of the input and output of the plant $(\mathbf{u}, \mathbf{y})$:

- Determine whether the consistency set $\mathscr{T}(\mathbf{y})$ is nonempty, with $\mathscr{T}(\mathbf{y}) \doteq \{g \in \mathscr{S}: \{y_k - (g * u)_k\}_{k=0}^{N} \in \mathscr{N}\}$.
- If $\mathscr{T}(\mathbf{y}) \neq \emptyset$, find a model $g_{id} \in \mathscr{T}(\mathbf{y})$ and a bound on the worst-case identification error.

In the sequel, we consider the following characterizations of the a priori set $\mathscr{S}_{np}$:

$$\mathscr{S}_{np1} \doteq \mathscr{B}\mathscr{H}_{\infty,\rho}(K) \quad \text{for some given } \rho \geqslant 1, \; K > 0, \tag{1}$$

$$\mathscr{S}_{np2} \doteq \{H(z) \in \mathscr{H}_{\infty,\rho}: |h_k| \leqslant K\rho^k, \forall k\}. \tag{2}$$

The first case above leads to a computable necessary and sufficient condition for checking consistency. However, in the case of unstable plants (as opposed to marginally stable), it may be difficult to check its validity. On the other hand, while characterization (2) is easily testable, as we will show in the next section, it leads only to sufficient conditions.

3.2. Consistency

Notice that an interpolatory algorithm such as the one proposed by Parrilo et al. (1999) can still be applied to establish consistency of the data and obtain an identified unstable model g_{id}, since stability of the unknown plant is used only to obtain worst-case error bounds and establish convergence. More precisely, there exists at least one model $g = h + p$ in $\mathscr{S}$ with $h \in \mathscr{S}_{np1}$ which can reproduce the experimental data within the assumed error bounds if and only if there exist two vectors $\mathbf{p} = [p_1 \cdots p_{N_p}]^{\mathrm{T}}$ and $\mathbf{h} = [h_0 \cdots h_N]^{\mathrm{T}}$ so that the following LMIs in $(\mathbf{p}, \mathbf{h})$ hold:

$$\mathbf{M}_R(\mathbf{h}) = \begin{bmatrix} \mathbf{R}_\rho^2 & \frac{1}{K}\mathbf{T}_h^{\mathrm{T}} \\ \frac{1}{K}\mathbf{T}_h & \mathbf{R}_\rho^{-2} \end{bmatrix} \geqslant 0,$$

$$\mathbf{y} - \mathbf{T}_u\mathbf{P}\mathbf{p} - \mathbf{T}_u\mathbf{h} \in \mathscr{N}, \tag{3}$$

where $(\mathbf{P})_k \doteq [g_k^1 \, g_k^2 \cdots g_k^{N_p}]$, $\mathbf{R}_\rho \doteq \mathrm{diag}\,[1\,\rho \cdots \rho^N]$, g_k^i denotes the kth Markov parameter of the ith transfer function $G_{p_i}(z)$ and h_k is the kth Markov parameter of the nonparametric component $H(z)$. The set of all models consistent with both the a priori assumptions and the a posteriori experimental data can be parametrized in terms of a free parameter $B(z) \in \mathscr{B}\mathscr{H}_\infty$. In particular, the choice $B(z)=0$ leads to the central model $G_{id}(z) = H_{id}(z) + \mathbf{p}^T\mathbf{G}_p(z)$ where an explicit state-space realization of $H_{id}(z)$ is given by

$$\mathbf{X} = \mathbf{C}_-^T\mathbf{C}_- + (\mathbf{A}^T - \mathbf{I})\mathbf{M}_R,$$

$$\mathbf{A}_H = \rho[\mathbf{A} - \mathbf{X}^{-1}\mathbf{C}_-^T\mathbf{C}_-(\mathbf{A} - \mathbf{I})]^{-1},$$

$$\mathbf{B}_H = \rho[\mathbf{C}_-^T\mathbf{C}_-(\mathbf{A}^T - \mathbf{A} - \mathbf{I}) - (\mathbf{A}^T - \mathbf{I})\mathbf{M}_R\mathbf{A}]^{-1}\mathbf{C}_-^T,$$

$$\mathbf{C}_H = K\mathbf{C}_+\{\mathbf{I} - [\mathbf{A} - \mathbf{X}^{-1}\mathbf{C}_-^T\mathbf{C}_-(\mathbf{A} - \mathbf{I})]^{-1}\},$$

$$\mathbf{D}_H = K\mathbf{C}_+[\mathbf{X}\mathbf{A} - \mathbf{C}_-^T\mathbf{C}_-(\mathbf{A} - \mathbf{I})]^{-1}\mathbf{C}_-^T,$$

with

$$\mathbf{A} = \begin{bmatrix} 0 & \mathbf{I}_{N\times N} \\ 0 & 0 \end{bmatrix},$$

$$\mathbf{C}_- = [\overbrace{1 \quad 0 \quad \dots \quad 0}^{N+1}], \qquad \mathbf{C}_+ = \frac{\mathbf{h}^T\mathbf{R}_\rho}{K}.$$

A potential problem here is that the condition number of $\mathbf{M}_R$ grows [1] as ρ^{4N}. This difficulty can be solved by noticing that if conditions (3) hold for some $K, \rho, \mathbf{h}$, then they hold for $K, \tilde{\rho}, \mathbf{h}_{\tilde{\rho}}$, with $\mathbf{h}_{\tilde{\rho}} \doteq [h_0\, h_1/\tilde{\rho} \cdots h_N/\tilde{\rho}^N]^T$. Thus, Problem 1 can be solved using the following scaled conditions:

$$\mathbf{R}_{\rho/\tilde{\rho}}^2 - \frac{1}{K^2}\mathbf{T}_{h_{\tilde{\rho}}}^T\mathbf{R}_{\rho/\tilde{\rho}}^2\mathbf{T}_{h_{\tilde{\rho}}} \geqslant 0$$

$$(\mathbf{R}_{\tilde{\rho}}^{-1}\mathbf{y} - \mathbf{T}_{\tilde{u}}\mathbf{P}_{\tilde{\rho}}\mathbf{p} - \mathbf{T}_{\tilde{u}}\mathbf{h}_{\tilde{\rho}}) \in \mathscr{N}_{\tilde{\rho}}, \tag{4}$$

where $\tilde{\rho} \sim \rho$, $\mathscr{N}_{\tilde{\rho}} \doteq \{\eta_{\tilde{\rho}}\colon |\eta_{\tilde{\rho}_k}| \leqslant \varepsilon/\tilde{\rho}^k\}$, $\mathbf{T}_{\tilde{u}} = \mathbf{R}_{\tilde{\rho}}^{-1}\mathbf{T}_u\mathbf{R}_{\tilde{\rho}}$ and $\mathbf{P}_{\tilde{\rho}} = \mathbf{R}_{\tilde{\rho}}^{-1}\mathbf{P}$, combined with the mapping $G_{id}(z) = G_{\tilde{\rho}}(z/\tilde{\rho})$. When $\tilde{\rho} > \rho$ the modified algorithm outlined above can be formally interpreted as solving the modified problem of obtaining a model of a *stable* plant in the set:

$$\mathscr{S}_{\tilde{\rho}} \doteq \{G_{\tilde{\rho}}(z) = G(\tilde{\rho}z), G \in \mathscr{S}\},$$

using the experimental data $\{u_k/\tilde{\rho}^k\}, \{y_k/\tilde{\rho}^k\}$, corrupted by noise in the set $\mathscr{N}_{\tilde{\rho}}$.

Remark 1. Since $\mathscr{S}_{np1} \subset \mathscr{S}_{np2}$, feasibility of the LMIs (4) also guarantees consistency of the a priori sets $(\mathscr{S}_{np2}, \mathscr{N})$ and the *a posteriori* experimental information $(\mathbf{u}, \mathbf{y})$. However, in this case the condition is clearly only sufficient.

While intuitively appealing, a difficulty with the approach outlined above is that neither the worst-case identification bounds obtained from the modified problem nor its convergence properties can be used to establish similar bounds or properties for the identified plant $G_{id}(z)$. However, as we show in the sequel, as long as $\tilde{\rho} > \rho$ then the identified model converges (in the ℓ_2 induced topology) to the actual plant as the information is completed.

3.3. Identification error and convergence properties

The identification procedure proposed above is interpolatory since it generates a model in the consistency set $\mathscr{T}(\mathbf{y})$. Thus, (see for instance Sánchez Peña & Sznaier, 1998, Chapter 10), its worst-case identification error can be bounded by:

$$e_{id} \doteq \sup_{\mathbf{y}\in\mathscr{Y}} \left\{ \sup_{g\in\mathscr{T}(\mathbf{y})} \|g - g_{id}(\mathbf{y})\|_{\ell_2[0,N]\to\ell_2[0,N]} \right\} \leqslant \mathscr{D}(\mathscr{I}), \tag{5}$$

where $g_{id}(\mathbf{y})$ denotes the model identified using the data $\mathbf{y}$, $\mathscr{Y}$ is the set of all possible experimental data consistent with the a priori information $(\mathscr{S}, \mathscr{N})$, and $\mathscr{D}(\mathscr{I}) \doteq \sup_{\mathbf{y}\in\mathscr{Y}} d(\mathscr{T}(\mathbf{y}))$ is known as the diameter of information. Moreover, since the a priori sets $(\mathscr{S}, \mathscr{N})$ are convex and symmetric, with points of symmetry $g_s = 0$ and $\eta_s = 0$, respectively, it can be shown (see Sánchez Peña & Sznaier, 1998) that the worst-case diameter is attained by experiments resulting a null output $\mathbf{y}_0$, i.e.:

$$\mathscr{D}(\mathscr{I}) = d(\mathscr{T}(\mathbf{y}_0)) = 2 \sup_{g\in\mathscr{T}(\mathbf{y}_0)} \|g\|_{\ell_2[0,N]\to\ell_2[0,N]}.$$

The following result provides an upper bound on the induced $\ell_2[0, N]$ norm of a not necessarily stable LTI system $G(z)$. This bound will be used to establish both, a worst-case bound on the identification error and convergence of the proposed method.

Lemma 2. *Consider a not necessarily stable LTI system g. Let $\tilde{\rho} > 1$ be such that the system $g_{\tilde{\rho}}$: $G_{\tilde{\rho}}(z) \doteq G(\tilde{\rho}z)$ is stable. Then $\|g\|_{\ell_2[0,N]\to\ell_2[0,N]} \leqslant \|G_{\tilde{\rho}}\|_\infty\tilde{\rho}^N$.*

Proof. Given in the appendix.

Corollary 3. *The worst-case identification error is bounded by*

$$e_{id} \leqslant 2\tilde{\rho}^N \left[\sum_{i=0}^{N} v_i + \|\mathbf{p}\|_\infty \sum_{i=1}^{N_p} \|(I - \mathscr{P}_N)g_{\tilde{\rho}}^i\|_{\ell_\infty\to\ell_\infty} + \frac{K(\rho/\tilde{\rho})^{N+1}}{1 - (\rho/\tilde{\rho})} \right], \tag{6}$$

where $v_i \doteq \min\{K(\rho/\tilde{\rho})^i + \|\mathbf{p}\|_\infty \sum_{i=1}^{N_p} |g_{\tilde{\rho},k}^i|, \|(\mathbf{T}_{\tilde{u}})_{i+1}^{-1}\|_1\varepsilon\}$, $\{g_{\tilde{\rho},k}^i\}$ is the kth Markov coefficient of the ith transfer function $G_{p_i}(\tilde{\rho}z)$ and $\|\mathbf{p}\|_\infty \doteq \|\mathbf{P}_{\tilde{\rho}}^\dagger\|_1(\|(\mathbf{T}_{\tilde{u}})^{-1}\|_1\varepsilon + K)$.

[1] This follows from the fact that $\bar{\sigma}(R_\rho^2) = \rho^{2N}$, $\underline{\sigma}(R_\rho^{-2}) = \rho^{-2N}$ and the interlacing property of the eigenvalues of symmetric matrices.

Proof. Follows from combining Lemma 2 with the error bound obtained in Parrilo et al. (1999).

Next we exploit this result to establish convergence of the algorithm when $N \to \infty$ and $\varepsilon \to 0$.

Theorem 4. *If $\tilde{\rho}$ is selected such that $\mathscr{S}_{\tilde{\rho}} \subset \mathscr{H}_\infty$, then the proposed algorithm is convergent, i.e.* $\lim_{\substack{N\to\infty \\ \varepsilon \to 0}} e_{id} = 0$.

Proof. Consider sequences $N_i \uparrow \infty$, $\varepsilon_i \downarrow 0$, and for a given pair (N, ε) denote by $\mathscr{T}(\mathbf{y}_0, N, \varepsilon)$ the set of plants consistent with the a priori information and the null outcome $\mathbf{y}_0$. Clearly if $g \in \mathscr{T}(\mathbf{y}_0, N, \varepsilon)$ then for $0 \leqslant k \leqslant N$ its kth Markov coefficient can be bounded by $|g_k| \leqslant \min\{\|(\mathbf{T}_u^{-1})_k\|_1 \varepsilon, K\rho^k + \|\mathbf{p}\|_\infty \sum_{j=1}^{N_p} |g_k^j|\}$. It follows that if, for every i, (N_i, ε_i) are selected such that $K\rho^{N_i} > \|(\mathbf{T}_u^{-1})_{N_i}\|_1 \varepsilon_i$ then $\mathscr{T}(\mathbf{y}_0, N_j, \varepsilon_j) \subset \mathscr{T}(\mathbf{y}_0, N_i, \varepsilon_i)$ for $j > i$,[2] and thus (Aubin & Frankowska, 1990, p. 18), the sequence of sets has a limit $\mathscr{T}^* = \bigcap_k \overline{\mathscr{T}(\mathbf{y}_0, N_k, \varepsilon_k)}$. If $\mathscr{T}^* \neq \{0\}$, then there exist some $g^* \in \mathscr{T}(\mathbf{y}_0, N_j, \varepsilon_j), \forall j$ and such that, for some M and ξ,

$$\|g^*\|_{\ell_2[0,M] \to \ell_2[0,M]} > \xi > 0. \tag{7}$$

Let $\mathscr{T}_{\tilde{\rho}}(\mathbf{y}_0, N_j, \varepsilon) = \{g_{\tilde{\rho}}\colon G_{\tilde{\rho}}(z) = G(\tilde{\rho}z), g \in \mathscr{T}(\mathbf{y}_0, N_j, \varepsilon)\}$. Since $g^*_{\tilde{\rho}} \in \mathscr{T}_{\tilde{\rho}}(\mathbf{y}_0, N_j, \varepsilon)$, $\forall j$, using the error bound derived in Parrilo et al. (1999), it follows that there exists some (N, ε) such that $\|g^*_{\tilde{\rho}}\|_\infty \leqslant \xi/\tilde{\rho}^M$. This, combined with Lemma 2 implies that $\|g^*\|_{\ell_2[0,M] \to \ell_2[0,M]} \leqslant \xi$, which contradicts (7). □

4. Examples

This section illustrates our theoretical results with two examples, one academic and one practical, the latter arising in the context of a computer vision application.

4.1. Example 1: A plant not strongly stabilizable

Consider the problem of identifying the following not strongly stabilizable plant, analytic in $|z| > 1.2223$:

$$S_1(z) = \frac{0.1009z^2 - 0.0002z - 0.1011}{z^2 - 0.4040z - 1},$$

from $N = 30$ samples of its impulse response corrupted by additive noise bounded in amplitude by $\varepsilon = 0.51$. Assume that there is some a priori knowledge about the approximate[3] location of the poles of the system. This information may be taken into account as a parametric *unstable* component of the model, by using the following basis functions:

$$\mathbf{G}(z) \doteq \left[\frac{z^2}{D(z)}, \frac{z}{D(z)}, \frac{1}{D(z)}\right]^{\mathrm{T}},$$

$$D(z) = z^2 - 0.4440z - 1.2076.$$

Choosing $\tilde{\rho} = 1.3444$[4] and using MATLAB's LMI Toolbox to find the minimum value of the worst case gain K of the nonparametric portion of the model so that the set of LMIs (4) was feasible, led to a nonparametric component with a stability margin $\rho = 0.9990$ and gain $K = 8.2249 \times 10^{-4}$. The corresponding coefficients of the parametric component of the model are $\mathbf{p} = [0.0512 - 0.0157 - 0.0670]^{\mathrm{T}}$. The actual plant, the identified unstable model and the experimental samples are shown in the upper plot of Fig. 1.

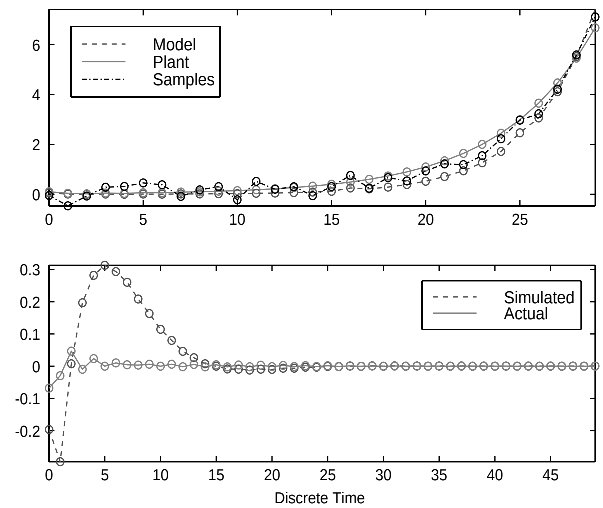

Fig. 1. (Upper) Identified model vs. plant. (Bottom) Controller on the model and actual plant.

These data can be directly used to synthesize a controller, if the goal is to guarantee performance over a *finite* horizon. On the other hand, since (6) tends to infinity as $M \to \infty$ it is not very useful for controller synthesis, when the goal is to guarantee performance over an infinite horizon. This difficulty can be solved by modelling the actual plant as the interconnection of the identified plant and stable dynamic uncertainty (for instance additive) and performing an additional model (in)validation step (Poolla, Khargonekar, Tikku, Krause, & Nagpal, 1994) to test the validity of the assumption and to quantify the size of this uncertainty. Since the proposed algorithm is convergent, one will expect that this invalidation will succeed, by taking N large enough and tightening the bounds in the experimental noise, if necessary. In this example, the invalidation step led to a bound on the magnitude of the (additive) uncertainty of $\|\Delta\|_\infty \leqslant 0.65$. The bottom plot of Fig. 1 shows the resulting controller. As

[2] For instance $g = K(\rho/z)^{N_i+1} \in \mathscr{T}(\mathbf{y}_0, N_i, \varepsilon_i)$ but $g \notin \mathscr{T}(\mathbf{y}_0, N_j, \varepsilon_j)$, $j > i$.

[3] To this end, the actual values of the poles were both perturbed by 10%.

[4] In this case, this a priori information is based on the approximate pole location of $\mathbf{G}(z)$.

Frame 8 Frame 14 Frame 19 Frame 21

Fig. 2. Robust identification based tracking (black cross) versus Mean Shift (white cross).

required, it stabilizes not only the nominal but the actual plant, and hence it can play the role of the prestabilizing controller required by most of the literature in the field.

If no a priori parametric information is available, the method outlined above can still be used, but at the expense of considering a larger number of data points. In this specific example, using $N = 50$ samples led to a model with gain of $K = 0.5995$, and closed-loop results similar to those shown in Fig. 1.[5]

4.2. Example 2: Multiframe tracking

A requirement common to most active vision applications is the *ability to track* objects in a sequence of frames. In principle, the location of the target can be predicted using a combination of its (assumed) dynamics, empirically learned noise distributions and past position observations (Blake & Isard, 1998). However, this process is far from trivial in a cluttered environment.

Fig. 2 shows the results of using a Mean Shift based tracking (white crosses) implemented in Intel's Open Source Computer Vision Library (Bradski & Pisarevsky, 2000). Although this algorithm is designed to improve tracking robustness by exploiting color information (Comaniciu, Ramesh, & Meer, 2000), it begins to track poorly in frame 19, and by frame 21 it has completely lost the target due to a combination of clutter and moderate occlusion. As we show next, this difficulty can be solved by modelling the motion of the target as the impulse response of an unknown nonSchur plant, and using the proposed approach to identify the relevant dynamics. Specifically, we considered as outputs the coordinates (x_k, y_k) of the centroid of the child in each frame, corrupted by noise bounded by $|\varepsilon| \leqslant 5.5$. This bound was quantified from fluctuations in the data taken when the person was at rest. For the sake of briefness we report below only the results for the x coordinate, since those for y are similar.

These assumptions can be taken into account by using as the parametric component of the model the span of $\mathbf{G}(z) \doteq [\frac{z^2}{z^2-2z+1}, \frac{z}{z^2-2z+1}]^{\mathrm{T}}$, combined with a nonparametric component, which explains the unmodelled dynamics, with $\rho = 0.99$. For tracking purposes, we selected the first $N = 12$ samples as training data in order to get a model of the person

Table 1
Id error as a function of k. Target width is 30 pixels

Sample	Mean-shift	ID-based	Worst-case bound
13	25.90	8.87	13
14	35.93	6.14	15
15	41.32	10.04	17
16	45.63	13.03	19
17	54.65	10.31	21
18	57.53	15.72	23
19	65.05	19.50	25
20	64.80	26.04	27

walking, using the technique proposed in Section 3.2. Both the consistency and identification problems were solved using MATLAB's LMI Toolbox, leading to $K_{\mathrm{opt}} = 1.35\mathrm{e}^{-12}$ and $\mathbf{p} = [127.7763 - 135.0723]^{\mathrm{T}}$. The advantage of this approach is illustrated in Fig. 2 where the black crosses indicate the position of the centroid predicted by our model. The numerical values of the error, computed as the difference between the predicted and actual values (using off-line image processing) are given in Table 1. As shown there, the identified model is able to predict the location of the target, far beyond the point where the mean shift tracker has failed.

Finally, notice that for this particular application the notion of identification error in terms of the largest difference between the predictions of any two models in the consistency set at $k > N$ (given a fixed known input) might be better suited than the one given by (5). More precisely, following Sections 3.2 and 3.3, let

$$e_{id}(k) \doteq \sup_{\mathbf{y}\in\mathscr{Y}} \left\{ \sup_{g\in\mathscr{T}(\mathbf{y})} |(g * u)_k - (g_{id}(\mathbf{y}) * u)_k| \right\}$$

$$\leqslant 2 \sup_{g\in\mathscr{T}(\mathbf{0})} \left| \left(\left(\sum_{i=1}^{N_p} p_i g^i + h \right) * u \right)_k \right|,$$

where the upper bound on the right hand side can be obtained as the solution to a Linear Programming problem in $\mathbf{p} = [p_1 \cdots p_{N_p}]^{\mathrm{T}}$ and $\mathbf{h} = [h_0 \cdots h_N]^{\mathrm{T}}$. The last column in Table 1 shows the error bounds as a function of k. As expected these values increase with time, since no new data is being used beyond $k = 12$. However, they became comparable with the width of the target (30 pixels) only beyond $k = 20$.

[5] The details, omitted for space reasons can be obtained by contacting the authors.

5. Conclusions

This paper addresses the problem of identifying nonSchur plants in a worst-case sense. Contrary to past work on this problem, the proposed method is intended to be applied in an open-loop setting. Thus it avoids the need for assumptions, such as the knowledge of a stabilizing controller for the unknown plant, that can prove to be too restrictive or even meaningless in many practical situations. In this sense, the contribution of the present paper can be viewed as twofold, on one hand by obtaining a model of an unstable plant in an open loop setting, and on the other, by getting a stabilizing controller, which together with the given model, constitute the first step in an iterative identification-design procedure such as the one proposed in e.g.: Hansen et al. (1989) and Schrama (1991).

Acknowledgements

This work was supported by NSF grants IIS-0117387 and ECS-0221562, and AFOSR grant F49620-00-1-0020.

Appendix A

A.1. Proof of Lemma 2

In order to proof Lemma 2 we need the following preliminary result:

Lemma 5. *Consider a LTI, stable system with state space realization*: $(\mathbf{A},\mathbf{B},\mathbf{C},\mathbf{D})$. *If the following functional LMI*:

$$\begin{bmatrix} \mathbf{A}^{\mathrm{T}}\mathbf{X}_{k+1}\mathbf{A}-\mathbf{X}_k+\mathbf{C}^{\mathrm{T}}\mathbf{C} & \mathbf{A}^{\mathrm{T}}\mathbf{X}_{k+1}\mathbf{B}+\mathbf{C}^{\mathrm{T}}\mathbf{D} \\ \mathbf{B}^{\mathrm{T}}\mathbf{X}_{k+1}\mathbf{A}+\mathbf{D}^{\mathrm{T}}\mathbf{C} & \mathbf{B}^{\mathrm{T}}\mathbf{X}_{k+1}\mathbf{B}-\gamma^2\mathbf{I}+\mathbf{D}^{\mathrm{T}}\mathbf{D} \end{bmatrix} < 0. \tag{A.1}$$

admits a solution $\mathbf{X}_k=\mathbf{X}_k^{\mathrm{T}} > 0$, *then* $\|h\|_{\ell_2[0,N]\to\ell_2[0,N]} < \gamma$.

Proof. Let $u\in\ell_2[0,N]$ denote an arbitrary input sequence and x, z the corresponding state and output sequences. Pre and post-multiplying (A.1) by $[\mathbf{x}_k^{\mathrm{T}}\ u_k]$ and $[\mathbf{x}_k^{\mathrm{T}}\ u_k]^{\mathrm{T}}$, and after some algebra gives:

$$0 > \mathbf{x}_{k+1}^{\mathrm{T}}\mathbf{X}_{k+1}\mathbf{x}_{k+1}+z_k^2-\mathbf{x}_k^{\mathrm{T}}\mathbf{X}_k\mathbf{x}_k-\gamma^2u_k^2.$$

Summing this last inequality from $k=0$ to $k=N$ and using the facts that $\mathbf{x}_0=0$ and $\mathbf{X}_k>0$, $\forall k$ yields:

$$0 > \mathbf{x}_{N+1}^{\mathrm{T}}\mathbf{X}_{N+1}\mathbf{x}_{N+1}+\sum_{k=0}^{N}(z_k^2-\gamma^2u_k^2)$$

$$\Rightarrow \sum_{k=0}^{N} z_k^2 < \gamma^2\sum_{k=0}^{N}u_k^2$$

which is equivalent to $\|h\|_{\ell_2[0,N]\to\ell_2[0,N]} < \gamma$. □

Proof of Lemma 2. Assume that g has a state space realization: $(\mathbf{A},\mathbf{B},\mathbf{C},\mathbf{D})$. Since $\|\tilde\rho^N G_{\tilde\rho}\|_\infty \leqslant \gamma\tilde\rho^N$, from the Bounded Real Lemma (see for instance Gahinet & Apkarian, 1994) there exists $\mathbf{X}_{\tilde\rho}=\mathbf{X}_{\tilde\rho}^{\mathrm{T}}>0$ such that

$$\begin{bmatrix} \mathbf{A}_{\tilde\rho}^{\mathrm{T}}\mathbf{X}_{\tilde\rho}\mathbf{A}_{\tilde\rho}-\mathbf{X}_{\tilde\rho}+\tilde\rho^{2N}\mathbf{C}^{\mathrm{T}}\mathbf{C} & \mathbf{A}_{\tilde\rho}^{\mathrm{T}}\mathbf{X}_{\tilde\rho}\mathbf{B}_{\tilde\rho}+\tilde\rho^{2N}\mathbf{C}^{\mathrm{T}}\mathbf{D} \\ \mathbf{B}_{\tilde\rho}^{\mathrm{T}}\mathbf{X}_{\tilde\rho}\mathbf{A}_{\tilde\rho}+\tilde\rho^{2N}\mathbf{D}^{\mathrm{T}}\mathbf{C} & \mathbf{B}_{\tilde\rho}^{\mathrm{T}}\mathbf{X}_{\tilde\rho}\mathbf{B}_{\tilde\rho}+\tilde\rho^{2N}(\mathbf{D}^{\mathrm{T}}\mathbf{D}-\gamma^2\mathbf{I}) \end{bmatrix} < 0$$

with $\mathbf{A}_{\tilde\rho}\doteq\mathbf{A}/\tilde\rho$ and $\mathbf{B}_{\tilde\rho}\doteq\mathbf{B}/\tilde\rho$. Define $\mathbf{X}_k\doteq\mathbf{X}_{\tilde\rho}\tilde\rho^{-2k}$. Multiplying last inequality by $\tilde\rho^{-2k}$, it follows that $\mathbf{X}_k$ satisfies:

$$\begin{bmatrix} \mathbf{A}^{\mathrm{T}}\mathbf{X}_{k+1}\mathbf{A}-\mathbf{X}_k+\mathbf{C}^{\mathrm{T}}\mathbf{C} & \mathbf{A}^{\mathrm{T}}\mathbf{X}_{k+1}\mathbf{B}+\mathbf{C}^{\mathrm{T}}\mathbf{D} \\ \mathbf{B}^{\mathrm{T}}\mathbf{X}_{k+1}\mathbf{A}+\mathbf{D}^{\mathrm{T}}\mathbf{C} & \mathbf{B}^{\mathrm{T}}\mathbf{X}_{k+1}\mathbf{B}-\gamma^2\tilde\rho^{2N}\mathbf{I}+\mathbf{D}^{\mathrm{T}}\mathbf{D} \end{bmatrix} + \gamma^2\tilde\rho^{2N}(1-\tilde\rho^{-2k})\begin{bmatrix} 0 & 0 \\ 0 & \mathbf{I} \end{bmatrix} + (\tilde\rho^{2(N-k)}-1)\begin{bmatrix} \mathbf{C}^{\mathrm{T}} \\ \mathbf{D}^{\mathrm{T}} \end{bmatrix}[\mathbf{C}\quad \mathbf{D}] < 0. \tag{A.2}$$

The proof follows now from Lemma 5 by noting that, since $\tilde\rho>1$, for $k\leqslant N$, condition (A.2) implies (A.1) □

References

Aubin, J. P., & Frankowska, H. (1990). *Set-valued analysis*. Boston: Birkhäuser.

Blake, A., & Isard, M. (1998). Condensation–condensation density propagation for visual tracking. *International Journal of Computer Vision*, *29*(1), 5–28.

Bradski, G. R., & Pisarevsky, V. (2000). Intel's computer vision library: Applications in calibration, stereo, segmentation, tracking, gesture, face and object recognition. *IEEE Computer Vision and Pattern Recognition (CVPR) II*, 796–797.

Chen, J., & Nett, C. (1995). The Carathéodory–Fejér problem and the $\mathscr{H}_\infty/\ell^1$ identification: A time domain approach. *IEEE Transactions on Automatic Control*, *40*(4), 729–735.

Comaniciu, D., Ramesh, V., & Meer, P. (2000). Real-time tracking of non-rigid objects using mean shift. *IEEE Computer Vision and Pattern Recognition (CVPR)*, 142–149.

Dasgupta, S., & Anderson, B. D. O. (1996). A parametrization for the closed-loop identification of nonlinear time-varying systems. *Automatica*, *32*(10), 1996.

Gahinet, P., & Apkarian, P. (1994). A linear matrix inequality approach to $\mathscr{H}_\infty$ control. *International Journal of Robust and Nonlinear Control*, *4*, 421–448.

Hansen, F., Franklin, G., & Kosut, R. (1989). Closed-loop identification via the fractional representation: Experiment design. In *1989 ACC*, Pittsburgh, PA, USA (pp. 1422–1427).

Mäkilä, P. M., & Partington, J. R. (1992). Robust identification of strongly stabilizable systems. *IEEE Transactions on Automatic Control*, *37*(11), 1709–1716.

Mäkilä, P. M., Partington, J. R., & Gustafsson, T. K. (1995). Worst-case control-relevant identification. *Automatica*, *31*(12), 1799–1819.

Parrilo, P. A., Sánchez Peña, R., & Sznaier, M. (1999). A parametric extension of mixed time/frequency robust identification. *IEEE Transactions on Automatic Control*, *44*(2), 364–369.

Partington, J. R., & Mäkilä, P. M. (1994). Worst-case analysis of identification—BIBO robustness for closed-loop data. *IEEE Transactions on Automatic Control*, *39*(10), 2171–2176.

Poolla, K., Khargonekar, P., Tikku, A., Krause, J., & Nagpal, K. (1994). A time domain approach to model validation. *IEEE Transactions on Automatic Control*, *39*(5), 951–959.

Sánchez Peña, R., & Sznaier, M. (1998). *Robust systems theory and applications*. New York: Wiley & Sons, Inc.

Schrama, R. J. P. (1991). Control-oriented approximate closed-loop identification via fractional representations. In *1991 ACC*, Boston, MA, USA (pp. 719–720).

Mario Sznaier received the Ingeniero Electronico and Ingeniero en Sistemas de Computacion degrees from the Universidad de la Republica, Uruguay in 1983 and 1984, respectively and the MSEE and Ph.D degrees from the University of Washington in 1986 and 1989, respectively. From 1991 to 1993 he was an Assistant Professor of Electrical Engineering at the University of Central Florida. In 1993 he joined the Pennsylvania State University, where he currently is a Professor of Electrical Engineering.

He has also held visiting appointments at the California Institute of Technology in 1990 and 2000.

His research interest include Multiobjective Robust Control; l1 and H-infinity. Control Theory, Control Oriented Identification and Active Vision.

María Cecilia Mazzaro received the Ingeniero Electrónico degree from the University of Buenos Aires, Argentina in 1997, where she was engaged in research activities until 1999. Since fall 1999 she is at the Pennsylvania State University, where she is a Research Assistant and a Ph.D. candidate. Her current research interests include system identification and model (in)validation, in particular its applications to visual analysis of human motion and tracking.

Octavia Camps received the B.S. degree in computer science and the B.S. degree in electrical engineering from the Universidad de la Republica (Montevideo, Uruguay) in 1981 and 1984, respectively, and the M.S. and Ph.D. degrees in electrical engineering from the University of Washington, in 1987 and 1992, respectively. In 1991, she joined the faculty at The Pennsylvania State University where she currently is an Associate Professor at the departments of Electrical Engineering and Computer Science and Engineering. In 2000, she was a visiting faculty at the California Institute of Technology and at the University of Southern California. Her current research interests include robust computer vision, pattern recognition, and image processing.